

## Analysis of Discontinuous Space Vector PWM Techniques for a Seven-Phase Voltage Source Inverter

Mohd. Arif Khan<sup>#1</sup>, Atif Iqbal<sup>#2</sup>, Sk Moin Ahmad<sup>#2</sup>, Zakir husain<sup>#3</sup>

<sup>#1</sup> Deptt. of Electrical & Electronics Engineering, Krishna Institute of Engg. &Tech., Ghaziabad, 201206, India,

<sup>#2</sup> Electrical & Computer Engineering Programme, Texas A&M University at Qatar, Doha, Qatar,

<sup>#3</sup> Department of Electrical & Electronics Engg, National Institute of Technology, Hamirpur, India

Email: mdarif27@rediffmail.com, atif2004@gmail.com, moin.nt@gmail.com, zahusain2@gmail.com

---

### Article Info

#### Article history:

Received Jan 4<sup>th</sup>, 2012

Revised Mar 20<sup>th</sup>, 2012

Accepted Mar 27<sup>th</sup>, 2012

---

#### Keyword:

DiscontinuousSVPWM

Space vector PWM

Total Harmonic Distortion

(THD)

Voltage Source Inverter (VSI)

---

### ABSTRACT

This paper presents discontinuous space vector PWM (DPWM) techniques for a seven-phase voltage source inverter (VSI). Space vector model of a seven-phase VSI shows that there exist 128 space vectors with different lengths and maps into fourteen sided polygons. A number of possibilities could arise to implement modulation of inverter legs due to large number of available space voltage vectors. Two strategies are adopted here; one utilising large and two middle sets of space vectors to implement discontinuous space vector PWM. Clamping of legs of inverter to either positive or negative dc bus leads to discontinuity in the switching and consequently offers reduced switching loss modulation strategy. A significant reduction in switching losses can be achieved while employing DPWM in a seven-phase VSI. A generalised method is also proposed to realize the DPWM in a seven-phase VSI. Comparison of continuous and discontinuous PWM is presented in terms of switching current ripple. The experimental set-up is illustrated and the experimental results are presented.

Copyright © 2012 Institute of Advanced Engineering and Science.

All rights reserved.

---

### Corresponding Author:

Mohd. Arif Khan,

Departement of Electrical and Electronics Engineering,

Krishna Institute of Engineering &Technology,

13<sup>th</sup> KM Stone, Ghaziabad-Meerut Road, Ghaziabad – 201206, INDIA

Email: [mdarif27@rediffmail.com](mailto:mdarif27@rediffmail.com)

---

## 1. INTRODUCTION

Speed controlled electric drives predominately utilise three-phase ac machines. However, since the variable speed ac drives require a power electronic converter for their supply, the number of machine phases is technically not limited. This has led to an increase in the interest in multi-phase (more than three-phases) ac drive applications, especially in conjunction with traction, EV/HEVs and electric ship propulsion [1]-[4]. Supply for multi-phase variable speed electric drive in the majority of cases is provided by Voltage Source Inverters. There are two methods of controlling the output voltage and frequency of such inverters namely; square wave mode and pulse width modulation mode. A number of PWM techniques are available to control a three-phase VSI [5]. However, Space Vector Pulse Width Modulation (SVPWM) has become the most popular one because of the easiness of digital implementation and better DC bus utilisation, when compared to the ramp-comparison sinusoidal PWM method. SVPWM for three-phase voltage source inverter has been extensively discussed in the literature [5]. SVPWM for a five-phase inverter is taken up in [6]-[13] and SVPWM for six-phase inverters are elaborated in [14]-[17]. Seven-phase inverter for a seven-phase brushless dc motor is illustrated in [18] and for axial flux seven-phase machine is presented in [19]. Continuous Space vector PWM to generate sinusoidal output from a seven-phase VSI is elaborated in [20]-[21]. Discontinuous space vector PWM technique for a seven-phase voltage source inverter is discussed in [22], where preliminary results are presented for method involving only two large outer set of vectors and with distorted output, in

contrast this paper proposes sinusoidal output case. More than seven-phase for instance nine-phase [23]-[25] and twelve phase [26] inverters are also available in the literature. Generalised space vector PWM for *n*-phase voltage source inverters is presented recently using duty ratio approach for sinusoidal output [27]. The analysis of output current ripples in multiphase drives using space vector approach is presented in [28]. Detailed review on the multiphase drive systems are presented in [29].

Switching losses are the main concern in multiphase drive systems as their major application areas are considered in high power range. The concept of discontinuity in switching legs can be employed as the potential means of reducing the switching losses [5]. Thus this paper analyses Discontinuous SVPWM technique to provide variable voltage and frequency output from a seven-phase VSI with reduced switching losses. This modulation technique is known to offer remarkable advantages compared to the continuous SVPWM in terms of significantly reduced switching losses. At first, in the paper modeling of a seven-phase VSI is reviewed in terms of space vector representation. The model obtained is decomposed into three two dimensional orthogonal spaces.

The switching combinations yield 128 space vectors spanning over fourteen sectors. Two different schemes are investigated in this paper. The outer large length space vectors are used to implement the Discontinuous SVPWM method at first followed by using six active space vectors. The six active vectors application yield sinusoidal output voltages and the other method produce low order harmonics in the output voltages. A comparison is done for the two schemes developed in the paper in terms switching current ripple. A generalised analytical expression is obtained and presented to access the switching loss reduction by adopting the discontinuous PWM schemes. Further a generalised concept is presented to generate the required leg voltages for discontinuous PWM schemes. Simulation and experimental results are provided to support the analytical and theoretical findings.

**2. MODELLING OF SEVEN-PHASE VSI**

Power circuit topology of a seven-phase VSI is shown in Fig. 1. Each switch in the circuit consists of two power semiconductor devices, connected in anti-parallel. One of these is a fully controllable semiconductor, such as a bipolar transistor or IGBT, while the second one is a diode. The input of the inverter is a dc voltage, which is regarded further on as being constant. The inverter outputs are denoted in Fig. 1 with lower case symbols (*a,b,c,d,e,f,g*) while the points of connection of the outputs to inverter legs have symbols in capital letters (*A,B,C,D,E,F,G*). A complete space vector model of a seven-phase VSI is reported in [19]. A brief review is presented here. The total number of space vectors available in a seven-phase VSI is  $2^7=128$ . Out of these 128 space voltage vectors, 126 are active and two are zero space vectors and they form nine concentric polygons of fourteen sides in d-q plane with zero space vectors at the origin as shown in Fig-2.

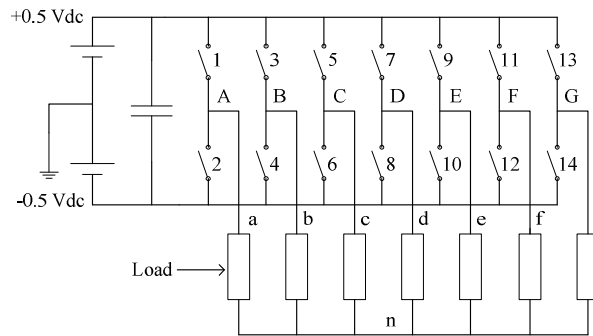


Figure 1 Seven-phase voltage source inverter power circuit

However, since a seven-phase system is under consideration, one has to represent the inverter space vectors in a seven-dimensional space. Such a space can be decomposed into three two-dimensional sub-spaces (*d-q*,  $x_1-y_1$  and  $x_2-y_2$ ) and one single-dimensional sub-space (zero-sequence). Since the load is assumed to be star-connected with isolated neutral point, zero-sequence cannot be excited and it is therefore sufficient to consider only three two-dimensional sub-spaces, *d-q*,  $x_1-y_1$  and  $x_2-y_2$ . Inverter voltage space vector in *d-q* sub-space is given with [20],

$$v_{dq} = (2/7) (v_a + av_b + a^2v_c + a^3v_d + a^*3v_e + a^*2v_f + a^*v_g) \tag{1a}$$

where  $a = e^{j2\pi/7}$ ,  $a^2 = e^{j4\pi/7}$ ,  $a^3 = e^{j6\pi/7}$  and \* stands for a complex conjugate.

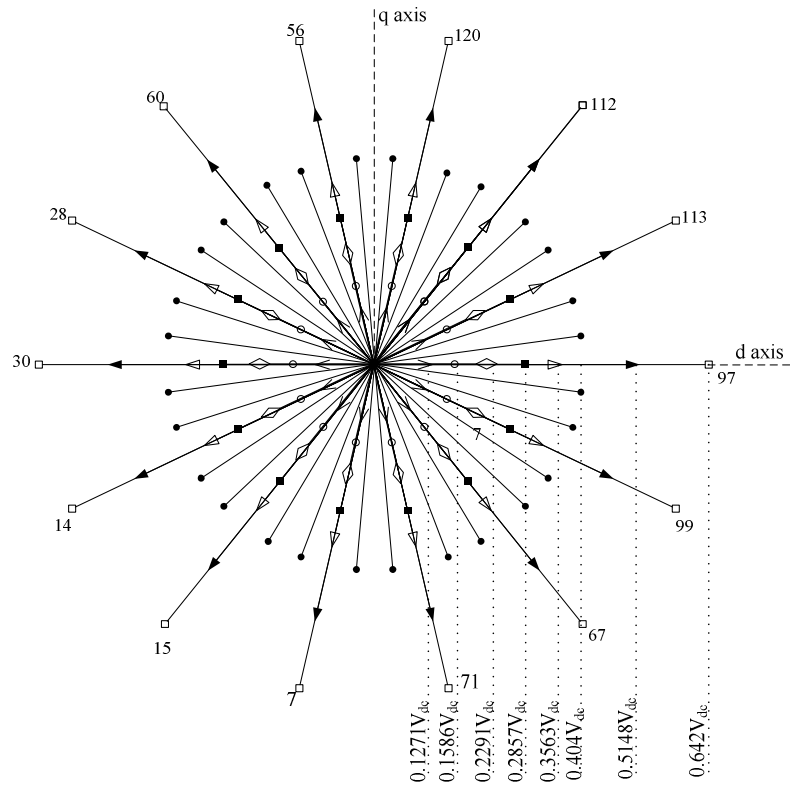


Figure 2 Phase-to-neutral voltage space vectors for states 1-128 (states127-128 are at origin) in  $d$ - $q$  plane

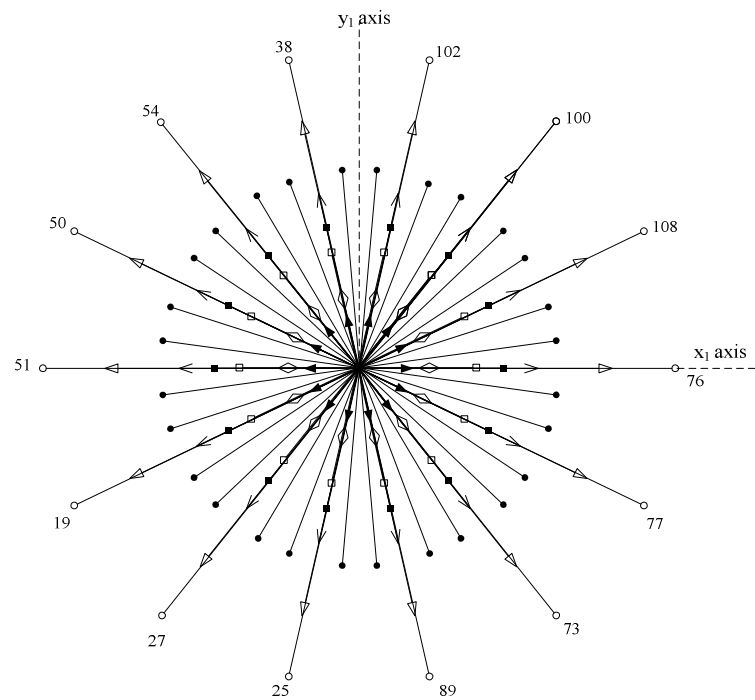


Figure 3 Phase-to-neutral voltage space vectors for states 1-128 (states127-128 are at origin) in  $x_1$ - $y_1$  plane

On the basis of the general decoupling transformation matrix for an  $n$ -phase system, inverter voltage space vectors in the second two-dimensional sub-space ( $x_1$ - $y_1$ ) and the third two-dimensional sub-space ( $x_2$ - $y_2$ ) are determined with,

$$\begin{aligned} v_{x1y1} &= (2/7)(v_a + a^2v_b + a^4v_c + a^6v_d + av_e + a^3v_f + a^5v_g) \\ v_{x2y2} &= (2/7)(v_a + a^3v_b + a^6v_c + a^2v_d + a^5v_e + av_f + a^4v_g) \end{aligned} \quad (1b)$$

The zero-sequence component is identically equal to zero because of the assumption of isolated neutral point. The phase voltage space vectors in two orthogonal planes, obtained using (1), are shown in Figs. 3 & 4.

It can be seen from Figs. 2, 3 and 4, the vector mapping in d-q axis, x1-y1 axis and x2-y2 axis. There are in total fourteen distinct sectors with  $25.714286^\circ$  ( $\pi/7$  radians) spacing. The inner-most space vectors in  $d-q$  plane are redundant and are therefore omitted from further discussion. This is in full compliance with observation of [17], where it is stated that only subset with maximum length vectors have to be used for any given combination of the switches that are 'on' and 'off' (3-4 and 4-3 in this case). The middle region space vectors correspond to two switches being 'on' from upper (lower) set and five switches being 'off' from lower (upper) set or vice-versa and one switch being 'on' from upper (lower) set and six switches being 'off' from lower (upper) set or vice-versa. In what follows, the vectors belonging to the middle region are simply termed medium and small vectors, while the vectors of the outer-most region are called large vectors.

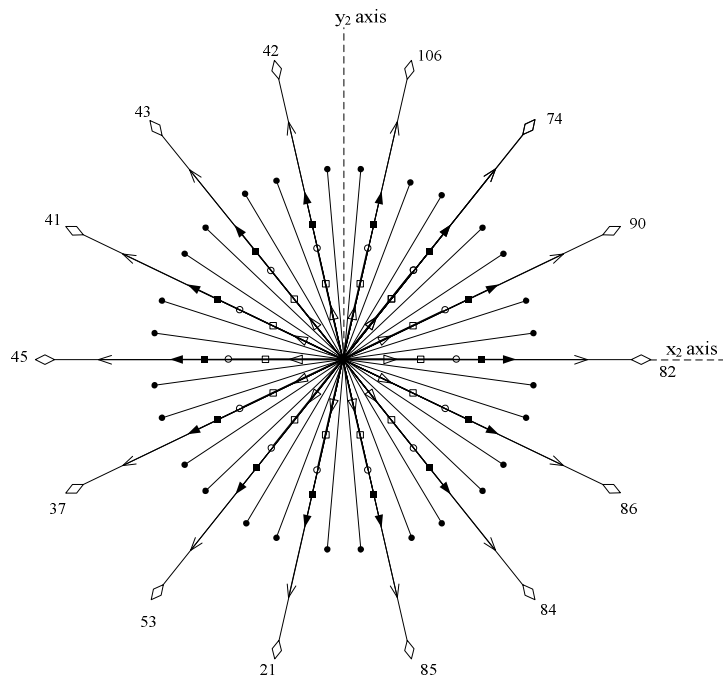


Figure 4 Phase-to-neutral voltage space vectors for states 1-128 (states 127-128 are at origin) in  $x_2$ - $y_2$  plane

### 3. CONTINUOUS SPACE VECTOR PULSE WIDTH MODULATION SCHEMES

#### 3.1. Using Only Large Vectors

This section reviews the continuous SVPWM schemes for a seven-phase VSI. Since there exist 128 space voltage vectors spanning in fourteen sectors, a large number of SVPWM schemes are possible. However, for simplicity only large vectors may be used to implement the SVPWM. The basic principle is to identify the location of reference voltage vectors and once it is known the two neighbouring large active vectors are applied for a specific time duration called dwell time and are given by;

$$t_a = \frac{|v_s^*| \sin(k\pi/7 - \alpha)}{|v_l| \sin(\pi/7)} t_s \quad (2a)$$

$$t_b = \frac{|v_s^*| \sin\left(\alpha - (k-1)\frac{\pi}{7}\right)}{|v_l| \sin(\pi/7)} t_s \quad (2b)$$

$$t_0 = t_s - t_a - t_b \quad (3a)$$

$$t_{127} = \gamma t_0 \quad (3b)$$

$$t_{128} = (1 - \gamma)t_0 \quad (3c)$$

where  $k$  is the sector number ( $k = 1$  to 14) and  $|v_{al}| = |v_{bl}| = |v_l| = \left(\frac{2}{7}\right) \frac{V_{DC}}{2 \cos(3\pi/7)} = 0.6419V_{DC}$ . Symbol  $v_s^*$

denotes the reference voltage space vector, while  $|x|$  stands for modulus of a complex number  $x$  and index “ $l$ ” stand for large vectors. Suffix ‘a’ stand for the vectors on the right of the reference vector and suffix ‘b’ refers to the active vector on the left of the reference vector.

It is to be noted that the factor  $\gamma$  offers a degree of freedom to formulate different types of PWM schemes. In case of continuous symmetrical SVPWM the factor  $\gamma = 0.5$  and in discontinuous SVPWM defined in the next section is either 0 or 1. The largest possible fundamental peak voltage magnitude that may be achieved using this scheme corresponds to the radius of the largest circle that can be inscribed within the tetra-decagon. The circle is tangential to the mid-point of the lines connecting the ends of the active space vectors. Thus the

maximum fundamental peak output voltage  $V_{\max}$  is  $V_{\max} = \left(\frac{2}{7}\right) \frac{V_{DC} \cos \frac{\pi}{14}}{2 \cos\left(\frac{3\pi}{7}\right)} = 0.6259V_{DC}$ . The maximum peak

fundamental output in fourteen-step mode is given with  $V_{14step} = \frac{2}{\pi} V_{DC} = 0.6366V_{DC}$  [24]. Thus the ratio of the maximum possible fundamental output voltage with SVPWM and in fourteen-step mode is  $V_{\max} / V_{\max,14step} = 0.9831583$ . The switching pattern for sector I is illustrated in Fig. 4, showing seven leg voltages. It is important to note that the three legs (A,B and G) have same pattern and three other legs (D,E and F) have same pattern. In other word it can be said that these legs are turned off simultaneously. The output voltage generated by this method contains a significant amount of lower order harmonic especially third and fifth. This is due to the fact that the  $x_1-y_1$  and  $x_2-y_2$  plane space vectors are not attenuated in the modulation scheme and are freely flowing.

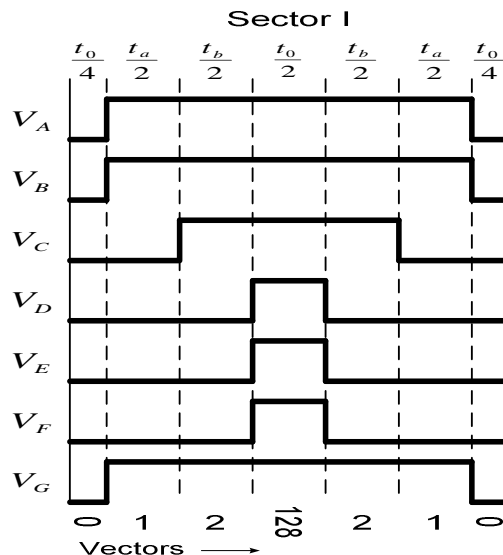


Fig. 4. Switching pattern and space vector disposition in sector I for SVPWM with large space vectors only.

### 3.2. Svpwm For Sinusoidal Output

The distributed winding machines require sinusoidal input voltage and current. Thus a method is devised to eliminate the lower order harmonics generated in the previous method. In essence it is essential to eliminate the unwanted space voltage vectors of  $x_1-y_1$  and  $x_2-y_2$  planes. The principle is to apply the required space vectors for appropriate time so that the  $x-y$  vector sets cancels each other. The times of applications of vectors are however, once again calculated using equations (2)-(3) with the following constraint;

$$\begin{aligned}
 t_a &= t_a^I + t_a^{II} + t_a^{III}; & t_b &= t_b^I + t_b^{II} + t_b^{III} \\
 t_a^{II} |v_{x1-y1}^{II}| + t_a^{III} |v_{x1-y1}^{III}| &= t_a^I |v_{x1-y1}^I|; & t_b^{II} |v_{x1-y1}^{II}| + t_b^{III} |v_{x1-y1}^{III}| &= t_b^I |v_{x1-y1}^I| \\
 t_a^{II} |v_{x2-y2}^{II}| + t_a^{III} |v_{x2-y2}^{III}| &= t_a^I |v_{x2-y2}^I|; & t_b^{II} |v_{x2-y2}^{II}| + t_b^{III} |v_{x2-y2}^{III}| &= t_b^I |v_{x2-y2}^I|
 \end{aligned}
 \tag{4}$$

Six active vectors are chosen from different sets in such a way that the corresponding vectors in the other two planes fall opposite to each other. With the constraint put by equation (4), these opposing vectors of  $x_1-y_1$  and  $x_2-y_2$  planes cancel each other. In this way sinusoidal output voltage is generated by the voltage source inverter. The space vector disposition and their respective magnitudes for sector 1 are illustrated in Fig. 5. The maximum available output voltage with this SVPWM method is  $0.513V_{dc}$ . Thus the ratio of the maximum possible fundamental output voltage with SVPWM and in fourteen-step mode is  $V_{max} / V_{max,14step} = 0.8058$ . The switching pattern for this scheme is elaborated in Fig. 6. It is noted from Fig. 6 that all the seven legs have staggered turning on and turning off times and thus have different switching pattern. This is actually the requirement of generating sinusoidal output.

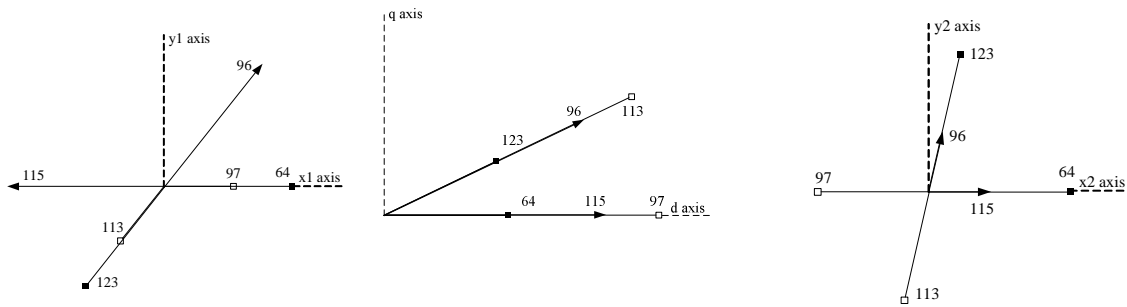


Fig. 5 Space vector disposition in sector 1 for sinusoidal output

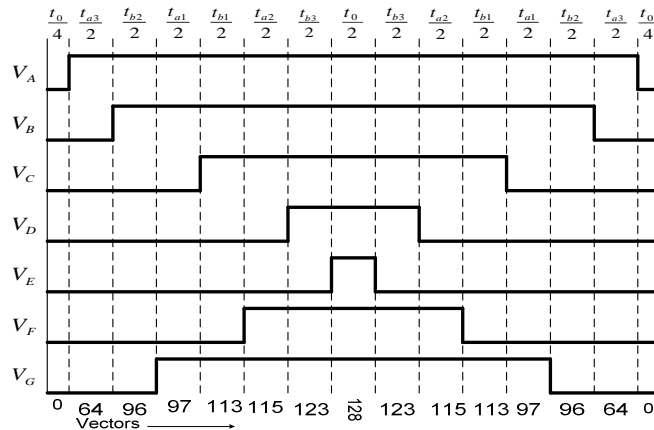


Fig. 6 Switching pattern and space vector disposition in sector I for sinusoidal SVPWM.

## 4. PROPOSED DISCONTINUOUS SVPWM

### 4.1 Using Only Large Vector [22]

This section describe the switching ripple characteristic in the discontinuities PWM method using only large vector, which was not presented in [22]. This is important for the comparison purposes. The

switchings of different legs are shown in Fig. 7 for DPWMMIN when using only large set of vectors, and the similar pattern can be evaluated in other DPWM schemes. The filled portion of Fig. 7, indicate the sectors where the corresponding leg remains un-modulated and the unfilled portion of the circle represents the time in which the switching takes place. It is evident that each leg remains un-modulated for six sectors (i.e. they are tied to the negative dc rail) and switches changes states in remaining eight sectors. It is also evident that in each sector three legs of the inverter remain un-modulated. In DPWMMIN and DPWMMAX the legs are tied continuously to either negative or positive dc rail, respectively in six sectors. In DPWM0 and DPWM1, the un-modulated legs changes alternatively in the two consecutive sectors.

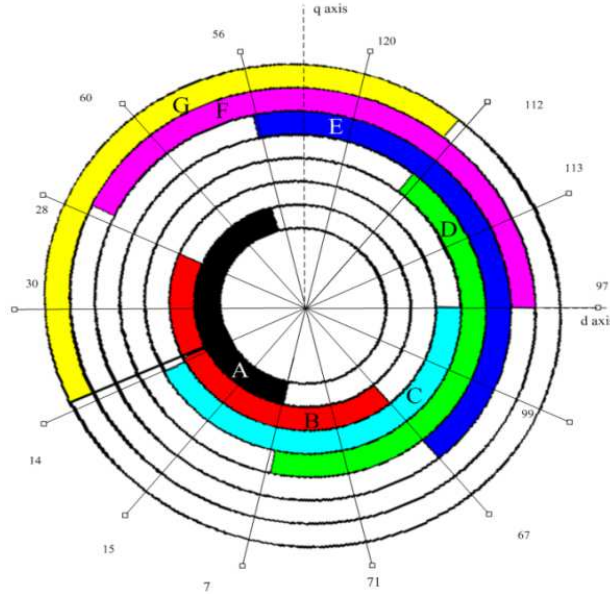


Fig. 7. Discontinuity in different legs during DPWMMIN.

*Current Ripple in DSVPWM*

The generalised current ripple equation is given as [5];

$$\tilde{i}_{ab}^2 = \left(\frac{V_{dc}}{L\sigma}\right)^2 \frac{T_s^2}{24} \left[ (u_2 - u_1)^2 + (u_2 - u_1)^3 + (u_2 - u_1)(u_2^3 - u_1^3) \right] \quad (5)$$

This equation is valid if  $\tilde{V}_{AB} = V_A - V_B > 0$  and in seven-phase case, it is only valid in sectors 4,5,6,11,12 & 13, i.e. in these sectors the difference between leg A and leg B voltage exist and in the rest of the sectors they are equal. With appropriate substitution for  $u_1$  and  $u_2$  for each modulation strategy the squared harmonic current ripple is evaluated.

As an example one sample calculation is shown here, for sector 4, part of the switching waveform is given in Fig. 8.

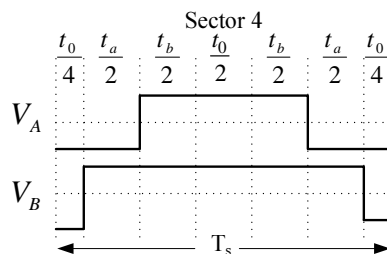


Fig. 8. Switching waveforms for the seven phase VSI in sector 4 using SVPWM in continuous mode.

The time of application in sector 4 is  $t_a = T_5$  and  $t_b = T_4$ . Considering  $V_A$  &  $V_B$ , average leg voltages

$$\begin{aligned} V_A &= \left( \frac{V_{dc}}{T_s} \right) [T_4 - T_5] \\ V_B &= \left( \frac{V_{dc}}{T_s} \right) [T_4 + T_5] \end{aligned} \quad (6)$$

The time of expression for each vector is substituted from equation (2) one gets;

$$\begin{aligned} V_A &= V_{dc} \left[ \frac{1}{\sin \frac{\pi}{7}} m \left( \cos \left( \frac{\pi}{14} + \alpha \right) + \sin \left( \frac{3\pi}{7} + \alpha \right) \right) \right] \\ V_B &= V_{dc} \left[ \frac{1}{\sin \frac{\pi}{7}} m \left( \cos \left( \frac{\pi}{14} + \alpha \right) - \sin \left( \frac{3\pi}{7} + \alpha \right) \right) \right] \end{aligned} \quad (7)$$

Now assuming;

$$u_1 = \frac{V_A}{V_{dc}}, u_2 = \frac{V_B}{V_{dc}} \quad (8)$$

Where  $m$  is the modulation index defined as;

$$m = \frac{|v_{out}|}{V_{14step}} \quad (9)$$

The current ripple expression for continuous mode is obtained as;

$$\tilde{i}_{ab}^2 = \int_{\frac{3\pi}{7}}^{\frac{4\pi}{7}} \tilde{i}_{ab}^2 + \int_{\frac{4\pi}{7}}^{\frac{5\pi}{7}} \tilde{i}_{ab}^2 + \int_{\frac{5\pi}{7}}^{\frac{6\pi}{7}} \tilde{i}_{ab}^2 + \int_{\frac{6\pi}{7}}^{\frac{3\pi}{7}} \tilde{i}_{ab}^2 + \int_{\frac{3\pi}{7}}^{\frac{2\pi}{7}} \tilde{i}_{ab}^2 + \int_{\frac{2\pi}{7}}^{\frac{3\pi}{7}} \tilde{i}_{ab}^2 \quad (10)$$

$$\tilde{i}_{ab}^2 = \left( \frac{V_{dc}}{L_\sigma} \right) \frac{T_s^2}{24} (0.120m^3 - 0.013m^2 + 0.016m - 0.005) \quad (11)$$

The current ripple expressions for discontinuous mode obtained as follows;

$$\tilde{i}_{ab}^2 = \left( \frac{V_{dc}}{L_\sigma} \right) \frac{T_s^2}{24} (0.118m^3 - 0.064m^2 + 0.068m - 0.003) \quad (12)$$

Or in more general terms as

$$\tilde{i}_{ab}^2 = \left( \frac{V_{dc}}{L_\sigma} \right)^2 \frac{T_s^2}{24} f(m) \quad (13)$$

Where the function  $f(m)$  is the *Harmonic distortion factor* (HDF). HDF is commonly used as a figure of merit for PWM strategies that are independent of switching frequency, DC bus voltage, and load inductances [5].

Where  $L_\sigma = L_1 + \frac{L_m L_2}{L_m + L_2}$ , and  $L_1, L_2, L_m$  correspond to stator leakage, rotor leakage, and the magnetizing inductances respectively. The current ripple is shown graphically for varying modulation index for continuous and discontinuous space vector PWM in Fig. 9. The ripple current in continuous SVPWM is seen lower than the discontinuous mode.

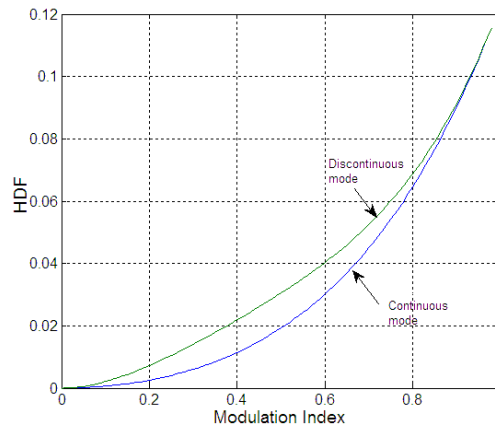
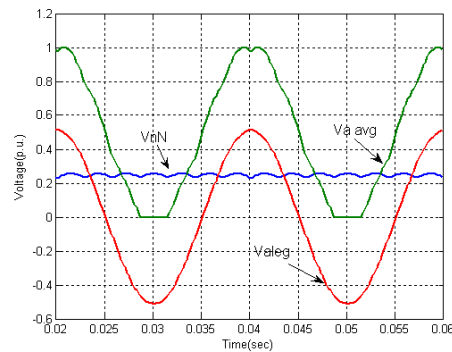
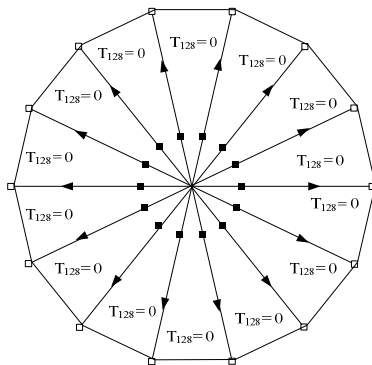


Fig. 9 Comparison between all the scheme on the basis of current ripple and modulation index

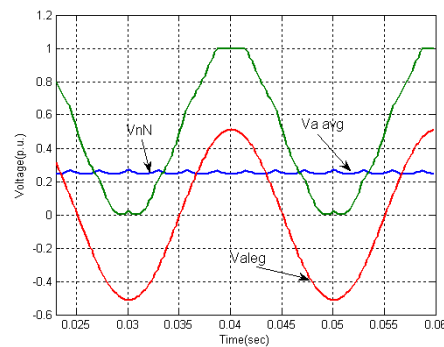
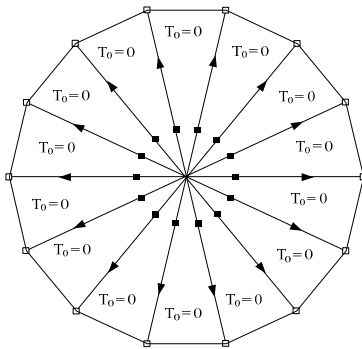
**4.2. Using Six Vector for Sinsusodial Output**

As a general rule the number of active vectors in space vector PWM for realising the sinusoidal output should be  $(n-1)$ . Hence in case of a seven-phase VSI, the number of active vectors should be 6 for realising sinusoidal output. The discontinuous space vector PWM is thus developed in this paper with the aim to generate sinusoidal output. The same principle as that of the last section is utilised to develop the discontinuous space vector PWM. The output phase voltages remains sinusoidal but the leg voltages and the common mode voltages takes different shapes depending on the type of the PWM techniques.

All the proposed schemes are presented in Fig 10, showing the placement of zero vectors and the waveforms for each schemes where  $V_{aleg}$  (Leg voltage),  $V_a$  (phase voltage),  $V_{nN}$  (voltage between neutral point). Once again only four different schemes are elaborated depending upon the relocation of the zero space vectors, nevertheless, a number of other possibilities do exist. The switching scheme is presented in Fig. 11 for DPWMMAX and DPWMMIN. It is observed that one leg remains unmodulated in contrary to the previously discussed method where three legs were unmodulated. Thus the number of switching is reduced to one seventh compared to its counterpart in continuous mode. The upper power switch remains continuously on and hence the leg is tied to the positive dc rail in DPWMMAX, while in DPWMMIN the lower power switch is continuously on leading to the leg being tied to the negative dc rail. To further show the discontinuity in different legs, another pictorial view is presented in Fig. 12, here the filled sector shows unmodulated legs. Thus each leg remains unmodulated for two consecutive sectors and modulates in remaining twelve sectors of the complete mapping.



a.



b.

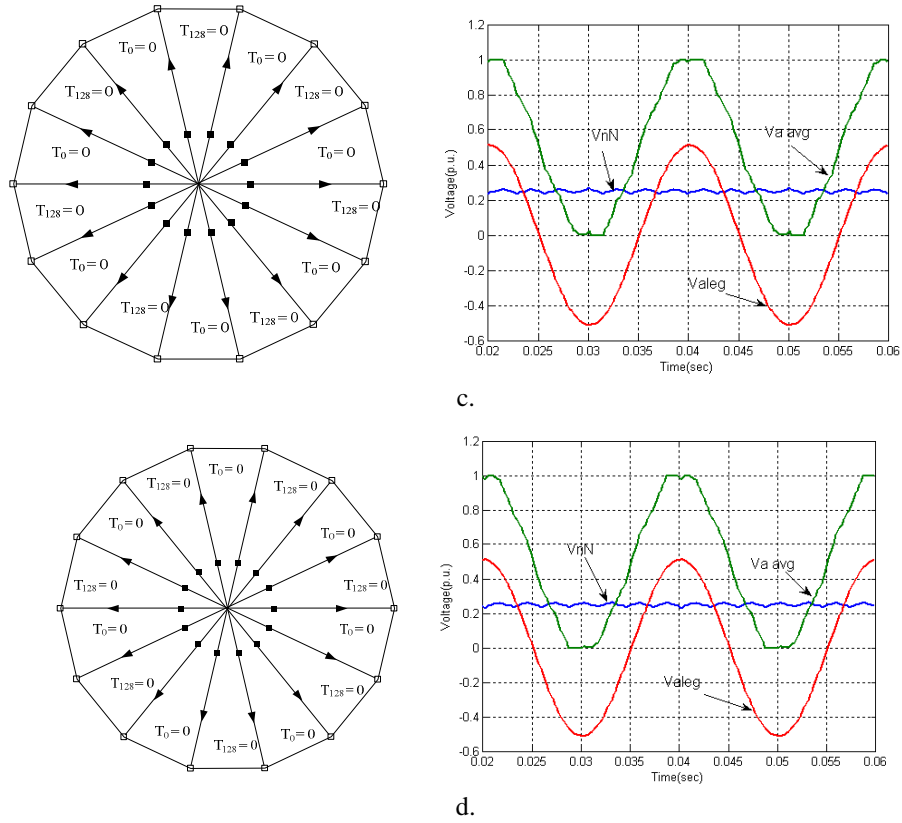


Fig. 10. Sinusoidal discontinuous PWM: a. DPWMMIN, b. DPWMMAX, c. DPWM0 and d. DPWM1.

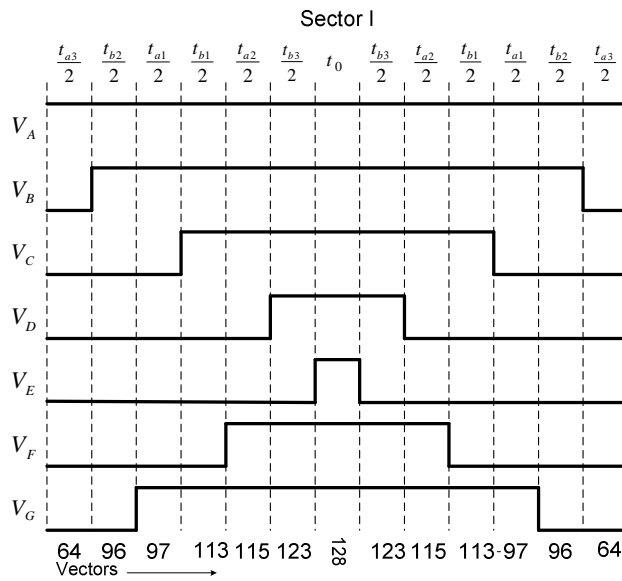


Fig. 11a. DPWM MAX for sector 1

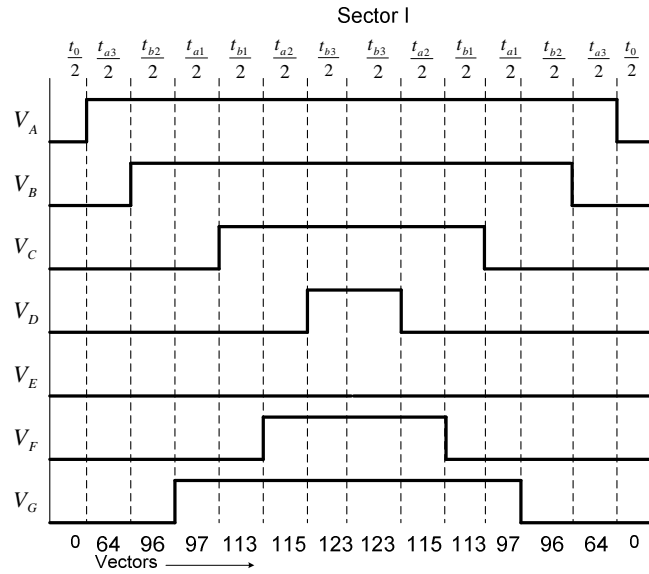


Fig. 11b. DPWM MIN for sector 1

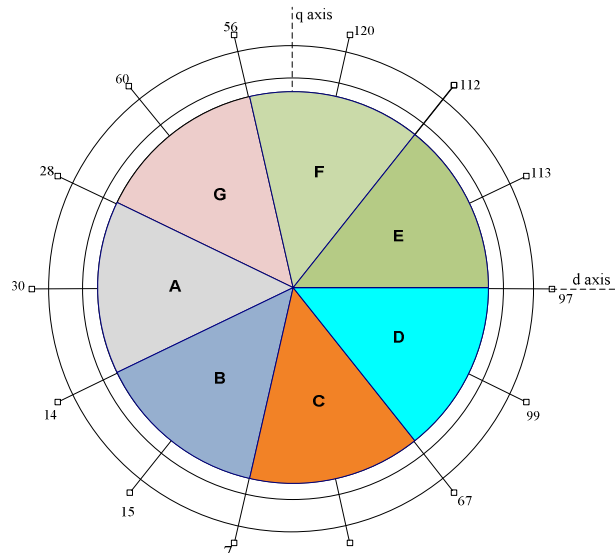


Fig. 12. Discontinuity in different legs during DPWMMIN

### Current Ripple in sinusoidal mode

For sector 1

$$V_A = V_{dc} \left[ \frac{1}{\sin \frac{\pi}{7}} m \left( \cos \left( \frac{5\pi}{14} + \alpha \right) + \sin(\alpha) \right) \right]$$

$$V_B = V_{dc} \left[ 0.0092m \left( 151 \cos \left( \frac{5\pi}{14} + \alpha \right) + 250 \sin(\alpha) \right) \right] \quad (14)$$

The square of the current ripple expression for the continuous mode

$$\tilde{i}_{ab}^2 = \left( \frac{V_{dc}}{L_\sigma} \right) \frac{T_s^2}{24} (1.354m^3 - 0.799m^2 + 0.141m - 0.006) \quad (15)$$

For DPWMMIN, DPWM0, mode it is obtained as;

$$\tilde{i}_{ab}^2 = \left(\frac{V_{dc}}{L_{\sigma}}\right) \frac{T_s^2}{24} (-0.04m^3 + 1.025m^2 - 0.229m + 0.010) \quad (16)$$

For DPWMMAX, DPWM1

$$\tilde{i}_{ab}^2 = \left(\frac{V_{dc}}{L_{\sigma}}\right) \frac{T_s^2}{24} (1.212m^3 + 0.268m^2 - 0.066m + 0.003) \quad (17)$$

The harmonic distortion is plotted in Fig. 13, shows once again lower distortion in the continuous mode. This is obvious due to the continuous switching in the inverter legs.

## 5. EXPERIMENTAL INVESTIGATION

Experimental investigation is performed to implement the proposed DPWM strategies for a seven-phase VSI. Three standard three-phase VSIs are used to provide seven-phase output. The DC link is paralleled to make it common for all the three modules. The DSP TMS320F2812 has provision of generating three independent PWM outputs per event manager by using full compare units and one independent PWM output is generated by the GP timer compare units. Thus a maximum of eight-phase inverter can be controlled using one DSP. The full compare unit has programmable dead-band for PWM output pairs but the other two PWM channels do not have the provision of dead band. Thus a dead band generating circuit is fabricated which act upon those PWM signals which do not have inbuilt dead band. A distribution panel is developed which distributes the fourteen PWM signals generated from DSP to three power modules. The schematic of a DSP based seven-phase VSI is presented in Fig. 14.

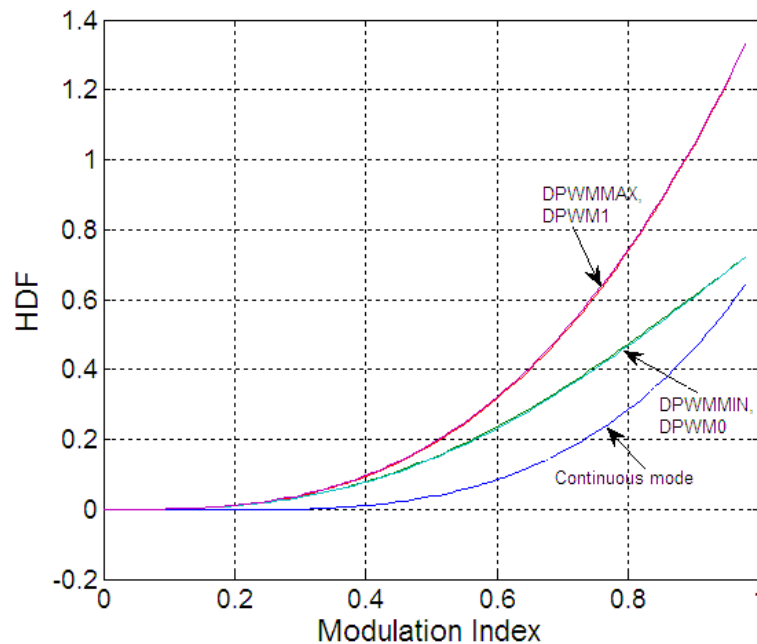


Fig. 13 Comparison between all the scheme on the basis of current ripple and modulation index

The experimental waveforms for sinusoidal output are illustrated in Fig. 15 for both DPWMMAX and DPWMMIN. In this case only one leg remain unmodulated and rest of the six legs switches as that of continuous space vector PWM case. The filtered leg voltages show either upper or lower cycle being flat due to discontinuity in the switching pattern. A seven-phase R-L load with  $R = 300$  watt and  $L = 24$  mH is connected to the inverter and the filtered phase voltages and load currents are depicted in the lower trace Fig. 16 for 50 Hz fundamental output and 10 kHz switching frequency. Tektronics current probe A622 is used to record the load current with scaling of 100mV/A. The phase voltage and current is sinusoidal as that of the continuous SVPWM. Thus the proposed discontinuous space vector PWM offer sinusoidal output with reduced switching losses and thus is recommended for use in medium voltage and high power applications.

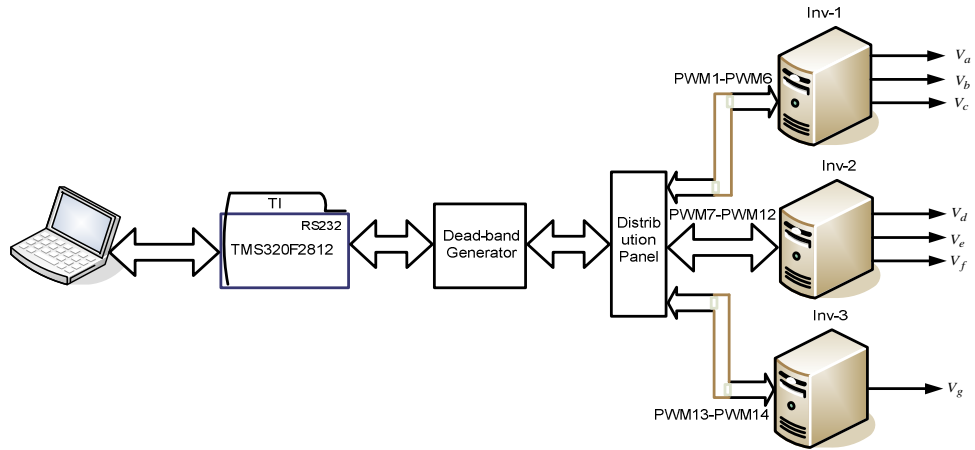


Fig. 14 Block schematic of a DSP based seven-phase VSI.

## 6. GENERALISED DISCONTINUOUS SVPWM

A generalised discontinuous Space vector PWM is available for a three-phase VSI in the literature. The same concept is extended here for a seven-phase VSI. A generalised neutral or common mode voltage is generated which is then injected into the reference voltage to obtain a set of modulating signals. These modulating signals are then compared with high frequency triangular wave to generate the gate drive signals. Although this is similar to carrier-based PWM method but it produces the output of the similar quality to that of the space vector PWM. The method can be explained using Fig. 16.

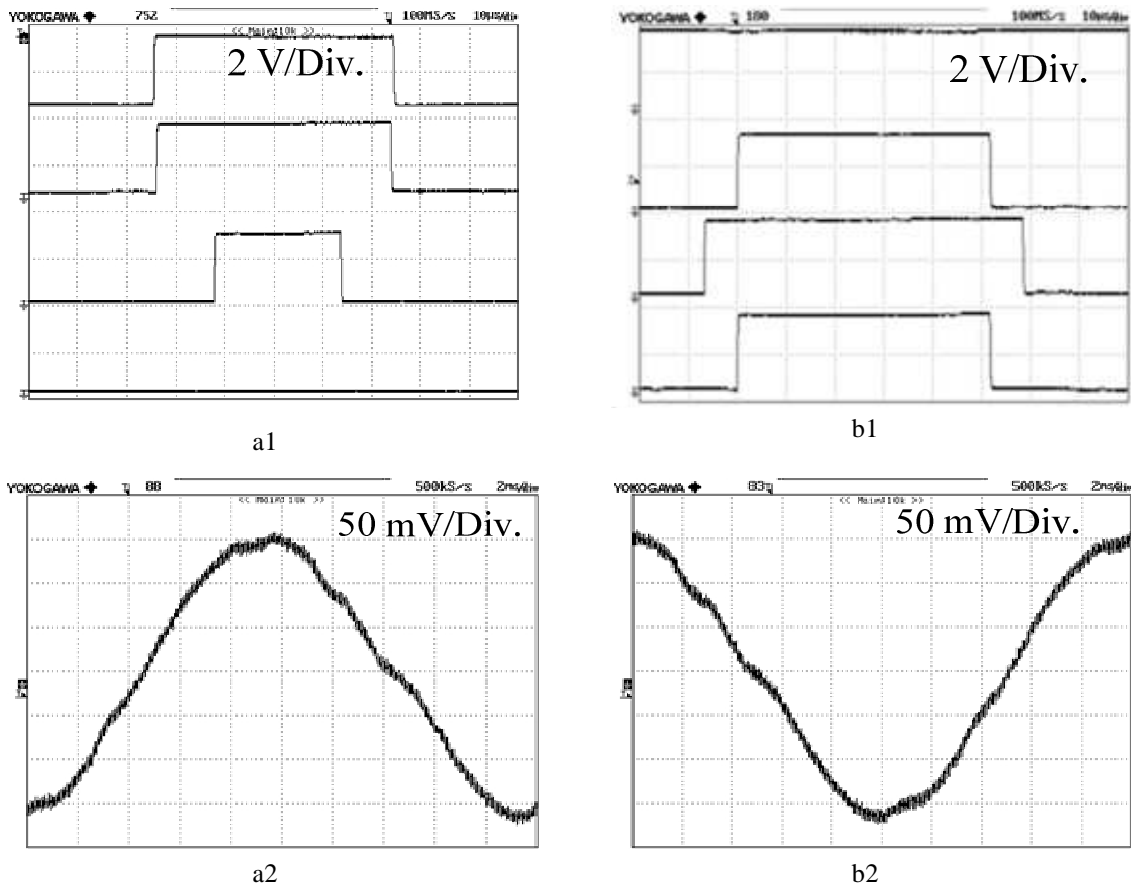


Fig. 15. Experimental waveform of DPWMMIN; a1. switching pattern and a2. filtered leg voltages for DPWMMIN, b1. switching pattern and b2. filtered leg voltage for DPWMMAX

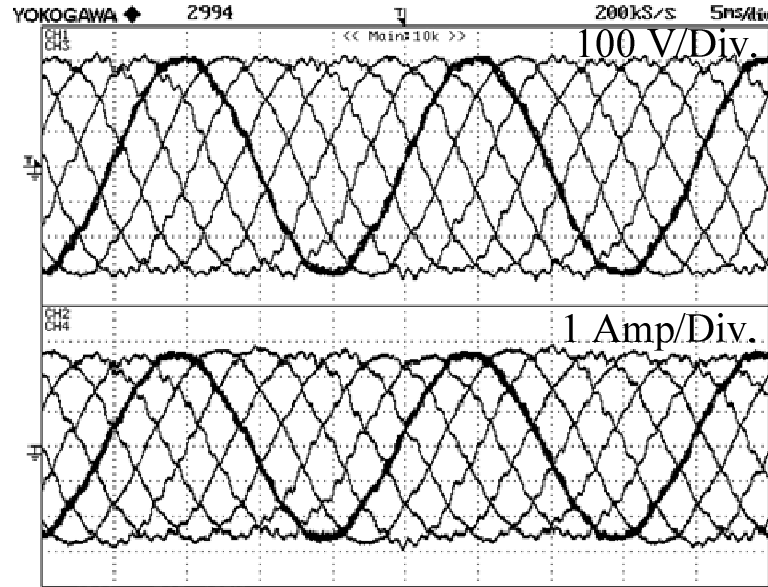


Fig. 16. Experimental waveform of filtered phase to neutral voltage and phase currents

Modulator phase angle is denoted by  $\alpha$  and is measured from the intersection point of the two reference wave at  $\alpha = \pi / 7$ . The common mode voltage shown as shaded portion in Fig. 15 is obtained as;

$$v_{nN} = \text{sgn}(v_a, v_b, v_c, v_d, v_e, v_f, v_g) * 0.5V_{dc} - \max(v_a, v_b, v_c, v_d, v_e, v_f, v_g) \quad (18)$$

At first the maximum reference voltage is identified and then the difference between the available dc bus voltage ( $0.5V_{dc}$ ) and the maximum of the reference yield common mode voltage. The control range of  $\alpha \rightarrow [0 - \pi / 7]$  to keep the operation of modulator in the linear range.

This concept can be generalised for  $k$ -phase voltage source inverter as given in equation (19) and the linear control range become  $\alpha \rightarrow [0 - \pi / k]$  ;

$$v_{nN} = \text{sgn}(v_a, v_b, v_c, \dots, v_k) * 0.5V_{dc} - \max(v_a, v_b, v_c, \dots, v_k) \quad (19)$$

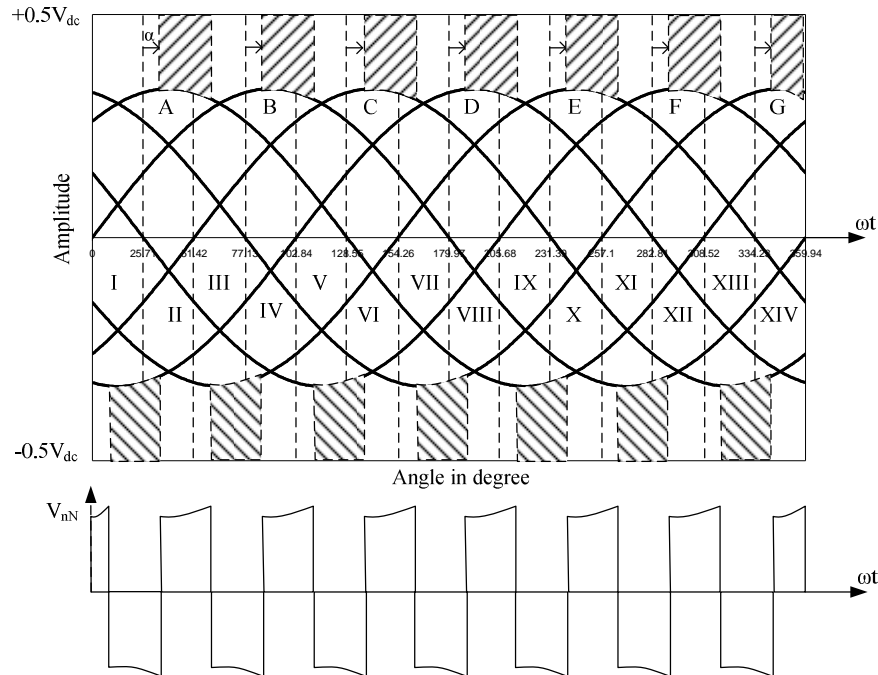


Fig. 17. Generalised Discontinuous PWM method for seven-phase VSI

## 7. CONCLUSION

This paper presents discontinuous space vector PWM schemes for a seven-phase voltage source inverter. Two methods are prevalent for implementing continuous space vector PWM, one using two large vectors and one using six space vectors, the latter offer sinusoidal output voltages. Thus this method is adopted in the paper to implement discontinuous space vector PWM method. Four different schemes are proposed and their behaviour is evaluated in terms of switching current ripple and compared with the existing continuous space vector PWM. The switching ripple is lower in case of continuous space vector PWM. However, switching losses will be lower in case of discontinuous space vector PWM as each leg remains unmodulated or not switched for two consecutive sectors. This leads to reduced switching but higher ripple. A generalised expression is presented to implement the discontinuous PWM for  $n$ -phase number. The distortion factor in switching currents is seen to be higher in discontinuous PWM mode due to lower number of switching in different legs of the inverter. The simulation and experimental results match to good extent.

## REFERENCES

- [1]. M.J. Duran, F. Sales, M.R. Arahal, "Bifurcation analysis of five-phase induction motor drives with third harmonic injection", *IEEE Trans. On Ind. Electr.* vol. 55, no. 5, May 2008, pp. 2006-2013.
- [2]. F. Barrero, M. R. Arahal, R. Gregor, S. Toral, and M. J. Duran, "One-step modulation predictive current control method for the asymmetrical dual three-phase induction machine", *IEEE Trans. On Ind. Electr.* vol. 56, no. 6, June 2009, pp. 1974-1983.
- [3]. F. Barrero, M.R. Arshal, R. Gregor and M.J. Duran, "A proof of concept study of predictive control for VSI driven symmetrical dual three-phase ac machines", *IEEE Trans. On Ind. Electr.* Vol. 56, no. 6, June 2009, pp. 1937-1954.
- [4]. M.G. Simoes, P. Vieira, "A high torque low speed multiphase brushless machine-A perspective application for electric vehicle", *IEEE Trans. Ind. Electr.*, Vol. 49, no. 5, Oct. 2002, pp. 1154-1164.
- [5]. G.D. Holmes, T.A. Lipo, "Pulse Width Modulation for Power Converters-Principle and Practice", IEEE Press-Series on Power Engineering, John Wiley and Sons, Piscataway, NJ, USA, 2003.
- [6]. A. Iqbal, E. Levi, "Space vector modulation scheme for a five-phase voltage source inverter", *Proc. European Power Electronics and Appl. Conf., EPE*, Dresden, Germany, 2005, CD-ROM paper 0006.
- [7]. A. Iqbal, E. Levi, "Space vector PWM techniques for sinusoidal output voltage generation with a five-phase voltage source inverter", *Electric Power Components and Systems*, vol. 34, no. 2, 2006, pp. 119-140.
- [8]. O. Ojo, G. Dong, Z.Wu, "Pulse width modulation for five-phase converters based on device turn-on times", *Proc. IEEE Ind. Appl. Soc. Annual Meeting IAS*, Tampa, FL, 2006, CD-ROM paper IAS15p7.
- [9]. H.M. Ryu, J.H. Kim, S.K. Sul, "Analysis of multi-phase space vector pulse width modulation based on multiple d-q space concept", *IEEE Trans. On Power Electronics*, vol. 20, no. 6, 2005, pp. 1364-1371.
- [10]. P.S. N. deSilva, J.E. Fletcher, B.W. Williams, "Development of space vector modulation strategies for five-phase voltage source inverters", *Proc. IEE Power Electronics, Machines and Drives Conf., PEMD*, Edinburgh, UK, 2004, pp. 650-655.
- [11]. H.A.Toliyat, M.M.Rahmian, T.A.Lipo, "Analysis and modelling of five-phase converters for adjustable speed drive applications", *Proc. 5th European Conference on Power Electronics and Applications EPE*, Brighton, UK, IEE Conf. Pub. No. 377, 1993, pp. 194-199.
- [12]. R.Shi, H.A.Toliyat, "Vector control of five-phase synchronous reluctance motor with space vector pulse width modulation (SVPWM) for minimum switching losses," *Proc. IEEE Applied Power Elec. Conf. APEC*, Dallas, Texas, 2002, pp. 57-63.
- [13]. H.A.Toliyat, R.Shi, H.Xu, "DSP-based vector control of five-phase synchronous reluctance motor," *IEEE Industry Applications Society Annual Meeting IAS*, Rome, Italy, 2000, CD-ROM paper no. 40\_05.
- [14]. Y. Zhao, T.A. Lipo, "Space vector PWM control of dual three-phase induction machine using vector space decomposition", *IEEE Trans. On Industry Applications*, vol. 31, no. 5, 1995, pp. 1100-1109.
- [15]. R.O.C. Lyra, T.A. Lipo, "Torque density improvement in a six-phase induction motor with third harmonic current injection" *IEEE Trans. On Industry Applications*, vol. 38, no. 5., 2002, pp. 1351-1360.
- [16]. D. Dujic, A. Iqbal, E. Levi, V. Vasic, "Analysis of space vector pulse width modulation for a symmetrical six-phase voltage source inverters", *Proc. Int. Power Conv. And Intelligent Motion Conf. PCIM*, Nurnberg, Germany, 2006, CD-ROM paper 154\_S6b-04\_Dujic.
- [17]. M.B.R. Correa, C.B. Jacobina, C.R. daSilva, A.M.N. Lima, E.R.C. daSilva, "Vector and Scalar modulation for six-phase voltage source inverters", *Proc. IEEE Power Elect. Spec. Conf. PESC*, Acapulco, Mexico, 2003, pp. 562-567.
- [18]. R.Dhawan and Z. Soghomonian, "Seven-phase brush-less synchronous motor with reduced inverter size," *Proc. Applied Power Electronics Conf. APEC*, Anaheim, CA, 2004 pp. 1099-1105.
- [19]. F. Locment, E. Semail, X. Ketelyn, A. Bouscayrol, "Control of seven-phase axial flux machine designed for fault operation", *Proc. IEEE Ind. Electr. Society Annual Meeting, IECON*, Paris, France, 2006, pp. 1101-1107.
- [20]. G. Grandi, G. Serra, A. Tani, "Space vector modulation of a seven-phase voltage source inverter", *Proc. Int. Symp. Power Electronics, Electrical Drives Automation and Motion SPEEDAM*, Taormina, Italy, 2006, CD-ROM paper S8-6.
- [21]. D. Dujic, M. Jones, G. Grandi, G. Serra, A. Tani, "Continuous PWM techniques for sinusoidal voltage generation with seven-phase voltage source inverter", *Proc. IEEE Power Electronics Specialist conf. PESC*, Orlando, FL, 2007, pp. 47-52.

- [22]. M. A. Khan, SK. M. Ahmed, A. Iqbal, H. Abu-Rub and S. Moinoddin, "Discontinuous space vector PWM strategies for a seven-phase voltage source inverter", *35<sup>th</sup> Annual Conf. Of the IEEE Ind. Elect. Society*, Porto, Portugal, Nov. 3-5, 2009.
- [23]. J.W. Kelly, E.G. Strangas, J.M. Miller, "Multi-phase space vector pulse width modulation", *IEEE Trans. On Energy Conversion*, vol. 18, no. 2, 2003, pp. 259-264.
- [24]. D. Dujic, M. Jones, E. Levi, "Space vector PWM for nine-phase VSI with sinusoidal output generation: analysis and implementation", *Proc. IEEE Ind. Elec. Society Annual Meeting, IECON*, Taipei, Taiwan, 2007, pp. 1524-1529.
- [25]. G. Grandi, G. Serra, A. Tani, "Space vector modulation of a nine-phase voltage source inverter", *Proc. IEEE Int. Symposium on Ind. Elect., ISIE*, Vigo, Spain, 2007, pp. 431-436.
- [26]. F. Yu, X. Zhang, H. Li, Z. Ye, "The space vector PWM control research of a multi-phase permanent magnet synchronous motor for electrical propulsion", *Proc. Int. Conf. on Elect. Machines & Systems, ICEMS 2003*, Bieging, China, pp. 604-607.
- [27]. D. Dujic, M. Jones, E. Levi, "Generalised space vector PWM for sinusoidal output voltage generation with multiphase voltage source inverters", *Int. Journal of Ind. Elect. And Drives*, vol. 1, NO. 1, 2009, pp. 1-13.
- [28]. D. Dujic, M. Jones, E. Levi, "Analysis of output current ripple rms in multiphase drives using space vector approach", *IEEE Trans. On Power Electronics*, vol. 24, NO. 8, August 2009, pp. 1926-1938.
- [29]. E. Levi, "Multiphase Electric Machines for variable speed applications", *IEEE Trans. On Ind. Elect.*, vol. 55, no. 5, May 2008, pp. 1893-1909.
- [30]. S. Moinuddin, A. Iqbal, "Modelling and simulation of a seven-phase VSI using Space Vector theory", *I Manager's Journal of Electrical Engg.*, vol. 1, no. 1, July-Sept. 2007, pp. 30-41.
- [31]. D C White and HH Woodson "Electromechanical Energy Conversion" MIT Press, New York, 1959.
- [32]. Atif Iqbal, Shaikh Moinuddin, "Analysis of space vector PWM techniques for a seven-phase voltage source inverter", *I Manager's Journal of Electrical Engg.*, vol. 1, no.2, Oct-Dec. 2007, pp. 53-63.

#### BIBLIOGRAPHY OF AUTHORS



**Mohd. Arif Khan** received his B.E. (Electrical) and M. Tech (Power System & Drives) degrees in 2005 and 2007, respectively, from the Aligarh Muslim University, Aligarh, India where he has submitted his PhD thesis. He has worked as Senior Research Fellow in a CSIR project, "Space Vector Pulse Width Modulation Techniques for Multiphase Voltage Source Inverter". Presently he is working with Krishna Institute of Engg. & Tech., Ghaziabad as Asstt. Prof. in EN deptt. His principal research interest is Multi-phase Multi-motor machine drives system.



**Atif Iqbal** received his B.Sc. and M.Sc. Engineering (Electrical) degrees in 1991 and 1996, respectively, from the Aligarh Muslim University, Aligarh, India and PhD in 2006 from Liverpool John Moores University, UK. He has been employed as Lecturer in the Department of Electrical Engineering, Aligarh Muslim University, Aligarh since 1991 and is working as Reader in the same university. Currently he is on academic pursuit and working with Deptt. of Electrical Engg., Qatar University, Doha, QATAR. He is recipient of Maulana Tufail Ahmad Gold Medal for standing first at B.Sc. Engg. Exams in 1991, AMU. His principal research interest is Power Electronics & Drives.



**Sk Moin Ahmed** born in 1983 at Hoogly, West Bengal. He received his B.Tech (Electrical) and M.Tech. (Power System & drives) in 2006 & 2008 respectively, from Aligarh Muslim University, Aligarh. He is gold medalist for securing top position in M.Tech. He is a recipient of Toronto fellowship funded by AMU. Currently he is pursuing his PhD at AMU.



**Zakir Husain** took his Bachelor and Master degrees in Electrical Engineering from Aligarh Muslim University, Aligarh, India. Subsequently he did his Ph.D from Motilal Nehru National Institute of Technology, Allahabad, India. He has been employed as Lecturer in the Department of Electrical Engineering since 1989 and is working as Associate Professor in the same the Institute. Currently he is on academic pursuit and working as Associate Professor and Head of Electrical Engineering Department, Salman Bin Abdul Aziz University, College of Engineering at Wadi Addawasir, Kingdom of Saudi Arabia. His principal research interest is Power System Engineering.